WALAILAK JOURNAL
http://wjst.wu.ac.th Information Technology

A New Algorithm to Detect Occluded Face from a Head Viewpoint using Hough Transform and Skin Ratio

Theekapun CHAROENPONG[*] and Patarida SANITTHAI

Department of Biomedical Engineering, Faculty of Engineering, Srinakharinwirot University, Nakhonnayok 26120, Thailand

([*]Corresponding author's e-mail: theekapun@gmail.com)

Received: 20 July 2014, Revised: 25 October 2014, Accepted: 26 November 2014

Abstract

The performance of current algorithms used in occluded face detection for surveillance systems is limited when detecting a face covered with an obstacle, or a non-frontal view of the face. Therefore, a method able to capture a face from any viewpoint is necessary. In this paper, we propose a new algorithm by using 2 subdivision regions and skin ratio for detecting occluded faces from any head viewpoint during +90 degrees to –90 degrees around the yaw axis. This algorithm consists of 3 steps: head region identification, skin extraction, and occluded face detection. First, the system is fed with an image sequence capturing the whole target body, to define the head region. The head region is detected using a blob technique under an experimental condition. Second, skin data is extracted, for computing skin ratio. Skin color is considered in multiple color spaces, and compared with a database by Mahalanobis Distance technique. Third, for occluded face detection, the human head area is equally divided into 2 vertical regions. The skin ratio of each part is used as a criterion for occlusion detection. To test the performance of the proposed algorithm, data from 35 subjects is used. The data of a subject is captured from any viewpoint of the head, varying from +90 degrees to −90 degrees. As this paper aims to develop surveillance systems, obstacles covering the whole face are focused on, such as helmets and masks. The accuracy rate of non-occluded face and occluded face detection is 98.81 and 94.90 %, respectively. The average accuracy rate is 95.39 %. The advantage of this method over recent research is that this is the first method to detect an occluded face from any viewpoint of the head varying from +90 degrees to –90 degrees.

Keywords: Surveillance system, multiple viewpoint occluded face detection, helmet detection, mask detection

Introduction

As crime or terrorism happens more frequently and strongly, a surveillance system is necessary in crime risk areas such as convenience stores, banks, shopping malls, and government buildings. A surveillance camera is a popular device widely used in such areas. The camera can record persons and their activities. Data from a surveillance camera can be used only in the case of an investigation. Therefore, a protection function that can detect a thief prior to the thief committing a crime needs to be included in the surveillance system. Occluded face detection is a solution to detect a potential thief. This work proposes an automatic system to identify persons who occlude their faces from any viewpoint of a head. Face occlusion is defined as being when the face is not able to be recognized or classified because of being covered by an obstacle, such as sunglasses, a mask, a helmet, a hat or a muffler, while a face without an obstacle is defined as being a normal face [1].

In previous works, view of face data and types of obstacle were considered. Some researchers proposed an occluded face detection method for general purposes of video surveillance application. Min *et al*. [2] proposed a scarf detection algorithm to classify the faces into 2 classes: the non-occluded face and the occluded face. The Gabor wavelet is applied for feature extraction. Forty filtered images from the Gabor wavelet are used as the features for classification. Principle component analysis (PCA) is used to reduce the feature data dimension. Support vector machines (SVM) classify the non-occluded face and the occluded face with a scarf. Frontal face image with scarf is used to test the proposed method. This method performs ineffectively for non-frontal face images, because only frontal face data was used as training set. Nirmala *et al*. [3] proposed a Mean Based Weight Matrix (MBWM) algorithm to enhance the performance of occluded face detection. The face image is segmented into 2 regions equally: an upper region and a lower region. A support vector machine is applied for occlusion detection classification. This study focuses on occluded face detection for a face covered only by a medical mask. The experiment is done by using a face image captured from the frontal position only. The accuracy rate is 98.75 % for detecting a face occluded with a medical mask. This research is not appropriate for detecting an occluded face from a non-frontal view, because the face feature is analyzed by the horizontal region.

Several studies have looked at Automated Teller Machines (ATMs) surveillance systems. Sang *et al*. [4] used support vector machines for detecting an occluded face while using the ATM. This method rejects a face occluded by sunglasses or scarf. The features of the non-occluded face and the occluded face are used to train the system. By integrating Principal Component Analysis (PCA) and SVM, the detected face is classified into a non-occluded face or an occluded face. Sunglasses and scarf are used in the experiment. The detection accuracies for sunglasses and scarf are 95.5 and 98.8 %, respectively. This research performs effectively for only frontal faces, because the face image is divided to 2 horizontal parts. Wen *et al*. [5] proposed a method to detect criminals while using an ATM. A circular shape detection method is applied to detect the helmet based on the Hough transform method. This method may not be appropriate for obstacles without a circular shape, such as a mask. Lin *at el*. [6] also proposed an assistant security system, by installing a camera near the ATM to detect an occluded face. The skin ratio, calculated from a frontal face image, is used to determine whether the face is covered with an obstacle or not. However, this method is restricted to data captured from the frontal viewpoint of the head. In the case where a face image is captured from other view, the skin ratio will be varied. Masks, hats, and helmets are used for face occlusion. Kim *at el*. [7] detected face occlusion when subjects wore sunglasses or masks. The input image is the upper part of body, including the shoulders and head. The edge is detected from the motion edge. The head and shoulders are separated by the ellipse fitting technique. Skin ratio is also used in this method. A mask occluding the mouth is used in the experiment. Skin ratio computed from the whole face is used as a criterion to classify the non-occluded and occluded face. Therefore, this method is not appropriate for application to an image of a face taken from multiple views.

An occluded face detection method is proposed for a specific purpose. Chiverton [8] proposed a helmet detection method for detecting a motorcycle rider, whether the rider wears helmet or not. An observed characteristic of a helmet, which is different from heads without a helmet, is the reflective property of the helmet, where the top of the helmet is brighter than the bottom half. However, it is difficult to ensure that light reflection on the helmet, with right position, can be captured in all images.

Our 2 related works previously proposed a method for detecting the occluded face. The first method uses the ellipse fitting method to define the head area in a still frontal face image [9]. Skin ratio is used to detect the occluded face. The input image focuses on frontal face data. Faces covered with helmets, masks, or sunglasses, and non-occluded faces, are used to test the performance of this method. We also solve the problem of the occluded face from only a frontal view by using 2 skin ratios [10]. A still face image with 5 different views was used in the experiment. Helmets, masks, and sunglasses were tested.

Current methods have limited applications to the real world, because of 3 problems: 1) performance in occluded face detection accuracy, 2) performance in detecting the occluded face with various types of obstacles, and 3) performance in detecting the occluded face image captured from multiple viewpoints of the head. In this paper, we propose an occluded face detection method by using Hough transform and skin ratios for face images captured from multiple viewpoints of the head. The faces are captured from any

viewpoint of the head between –90 degrees to +90 degrees around the yaw axis. As bank robbers usually wear helmets or masks to occlude their facial identities, this method is developed for detecting face occlusion by helmet and mask.

The remaining sections in this paper are organized as follows: the proposed method, experimental results, a discussion, and a conclusion in the last section.

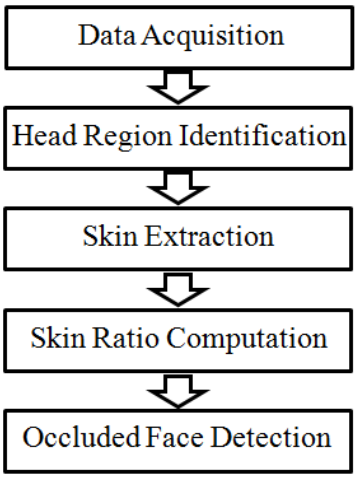

Figure 1 A diagram of occluded face detection. The occluded face detection method starts from data acquisition, head region identification, skin extraction, skin ratio computation, and occluded face detection.

The occluded face detection method

In this section, we describe a method of occluded face detection for any viewpoint of the head. The algorithm is shown in **Figure 1**. The whole body is captured in the format of image sequence. This algorithm consists of a 3 step process: head region identification, skin extraction, skin ratio computation, and occluded face detection. The following sections, including data acquisition, head region identification, skin extraction algorithm, skin ratio computation and occluded face detection will describe the occluded face detection algorithm in detail.

Data acquisition

The proposed method focuses on only the occluded face detection algorithm. Therefore, only one subject in the image is used as input data. The whole body of a subject, with a static background, is captured, as shown in **Figure 2a**. The camera is set far from the subject, at a distance of about 2.5 m and its position is at a height of 1.5 m from the floor. Light intensity along the walking way in the room, which the subject walks in during the data capture, is varied in a range of 275 - 393 lux. The subject turns around 360 degrees during recording of the face, from any viewpoint in an image sequence format file. The average turnaround speed is 5.62 s per round. Head viewpoint images varying from –90 degrees to +90 degrees are used in this research.

The –90 degrees head viewpoint involves the head turning to the right side, while +90 degrees involves the head turning to the left side. The frontal face is 0 degrees. The obstacles occluding the face are helmets, in red, dark blue, and brown colors, and masks, in black, red, dark blue, and brown colors. The non-occluded face is also collected in this data set.

Head region identification

As the whole human body is captured in an input image, this step aims to segment the head region by using blob technique and the Hough transform technique, as shown in **Figure 2**. The occluded face will be considered in the head region. Human features are extracted by a background subtraction technique. The human body is separated into more than one blob, as shown in **Figure 2b**. Each blob is represented by a different color. To define the head region, we find a blob with properties that correspond to 2 conditions for head region definition. First, the number of pixels in blobs must be larger than the criterion. Second, in such candidate blobs that correspond with the first condition, the blob center coordinate must be the highest in an image. The head region and head blob center are represented by a red blob, and a green square area as shown in **Figure 2b**, respectively. However, some head region blobs may include some parts of body, depending on background subtraction result. As the blob technique does not perform effectively, the Hough transform technique is then applied to make the head region more precise. The Cycle Hough transform is computed from the edge of the head region blob, as shown in **Figure 2c** and Eq. (1)

$$r(\theta) = x_i cos\theta + y_i sin\theta, \quad (1)$$

where (x_i, y_i) is the coordinate of the pixel on the edge of the head region.

The cycle size is radius r radius. A set of pixels along the edge from the top of head region blob is used for the Cycle Hough transform computation. After a cycle is computed, the head region is extracted more precisely, as shown by the yellow cycle in **Figure 2d**.

Skin extraction algorithm

In this section, skin face color is extracted for computing skin ratio. Many methods for skin color segmentation have been proposed [10-15]. Based on the robustness of skin color extraction, the most appropriate one, proposed by Singh and *et al*. [15], will be used in our skin color extraction step. Singh's method is robust for illumination conditions, because the brightness layer is not used for skin color extraction. Skin color is the combination result from the skin data that is extracted from only the chromatic layer of HSV, Lab and YC_BC_R color spaces. The 3 color spaces are converted from an RGB color image. Therefore, the layers that are considered for extracting the skin color extraction are the hue (H) and saturate (S) layers for HSV color space, the color-opponent dimensions (a and b) layers for Lab color space, and the blue-difference and red-difference (C_B and C_R) layers for YC_BC_R color space. For a layer, the skin color range has to be defined. We adapted the Mahalanobis distance technique and skin color database in Singh's method to define skin color range in a color layer, instead of using a constant range for global skin color. The skin extraction flowchart is shown in **Figure 3**. The strength of the algorithm has two points: 1) skin can be extracted effectively based on colors in the database, and 2) skin data is extracted from only the chromatic layer of HSV, Lab, and YC_BC_R color spaces; therefore, this method is robust for various levels of illumination conditions. However, for better performance of the skin extraction algorithm, skin color in the database should cover a wide range of skin color levels.

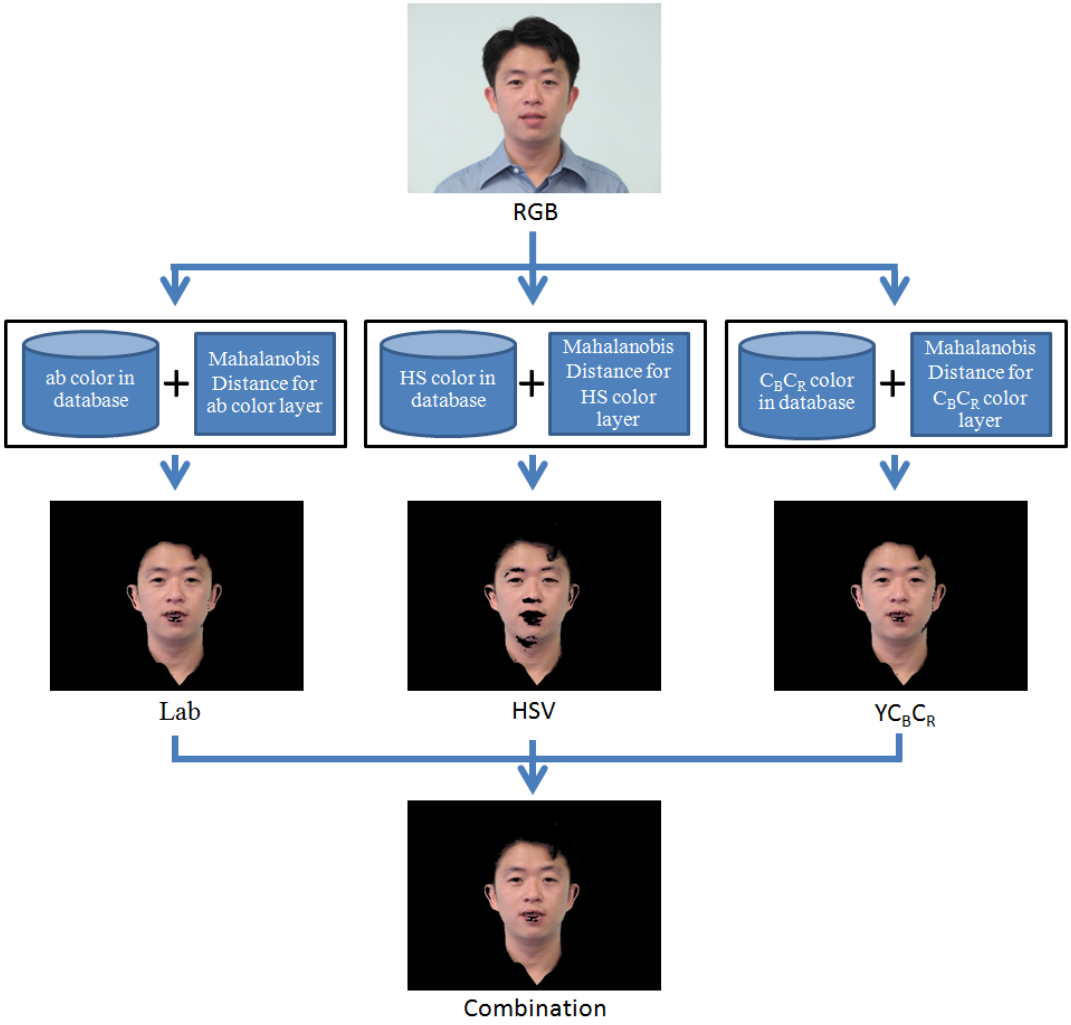

Figure 3 A skin color extraction flowchart. The input is an image in the RGB color space. The output is an image from a combination of 3 color spaces.

The Mahalanobis distance is applied for expressing multivariate normal distribution of the data. The distance of a pixel to the center is computed as;

$$r^2 = (x - \mu)^t \Sigma^{-1} (x - \mu), \quad (2)$$

where x is the pixel coordinate, μ is the mean vector, Σ is the covariance matrix, and r is the Mahalanobis distance from x to μ.

In **Figure 3**, the RGB image is converted into images in 3 color spaces: Lab, HSV, and YC_BC_R. The Mahalanobis distance of each color space is computed from the hue (H) and saturate (S) layer, the color-opponent dimensions (a and b) layer, and the blue-difference and red-difference (C_B and C_R) layer for YC_BC_R color space. A covariance matrix is defined from skin color in the database. Comparing the Mahalanobis distance criterion of each color space, the color which has a Mahalanobis distance located in the range of the Mahalanobis distance criterion is defined as a skin color space. Sample results of skin color from each color space are represented in an RGB color space, as shown in the third row of **Figure**

3. The fourth row shows a skin color result that has been combined from Lab, HSV, and YC_BC_R color space. The combined result shows a better result, rather than when just using a color space.

a) RGB image

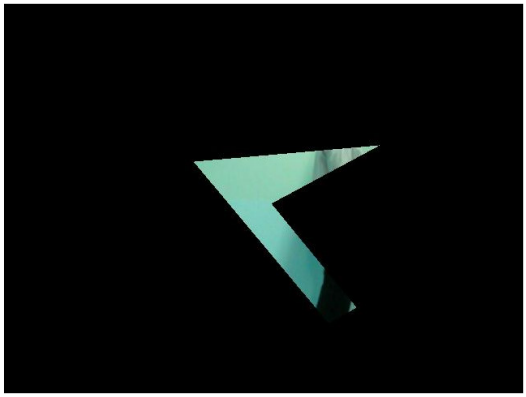

b) ROI

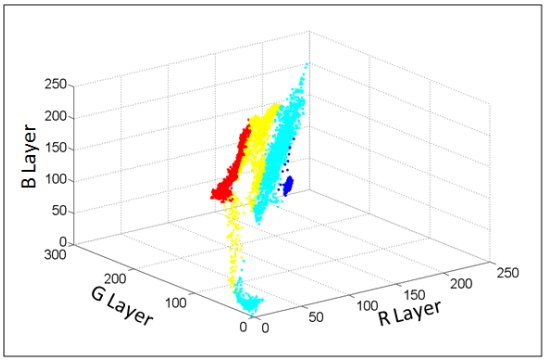

c) The Mahalanobis distance of skin color in an RGB space

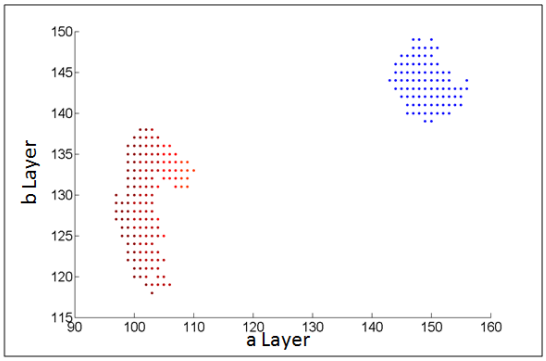

d) The Mahalanobis distance of skin color in ab space from a Lab color mode

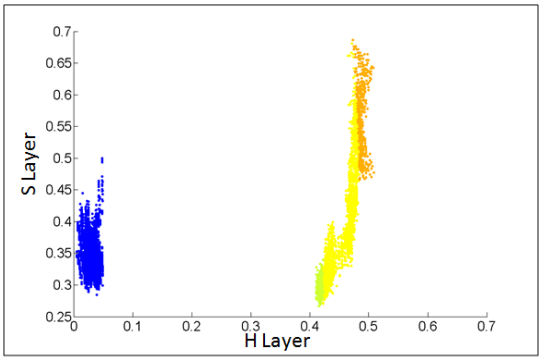

e) The Mahalanobis distance of skin color in an HS space from an HSV color mode

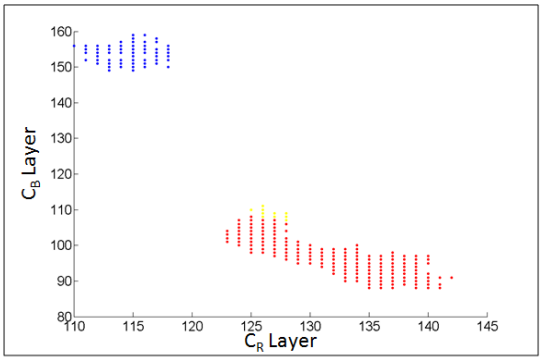

f) The Mahalanobis distance of skin color in a C_BC_R space from a YC_BC_R color mode

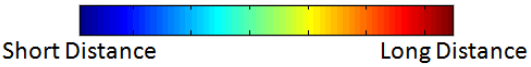

g) Color index for Mahalanobis distance ranges representation.

Figure 4 Mahalanobis distance results of skin and non-skin colors.

The Mahalanobis distance results of skin and non-skin colors is represented as per the graphic in **Figure 4**. Skin colors and non-skin colors are shown in RGB, Lab, HSV and YC_BC_R color spaces, as shown in **Figures 4c - 4f**, respectively. Non-skin colors are extracted from pixels in regions of interest (ROI) in **Figure 4a**, as shown in **Figure 4b**. Each range of the Mahalanobis distance is identified with different color bases on the color index in **Figure 4g**. Dark blue represents a short Mahalanobis distance, and dark red represents a long Mahalanobis distance. Obviously, skin color in RGB, ab, HS, and C_BC_R spaces are represented in a dark blue color, as shown in **Figures 4c - 4f**, respectively. Non-skin color is represented by other colors.

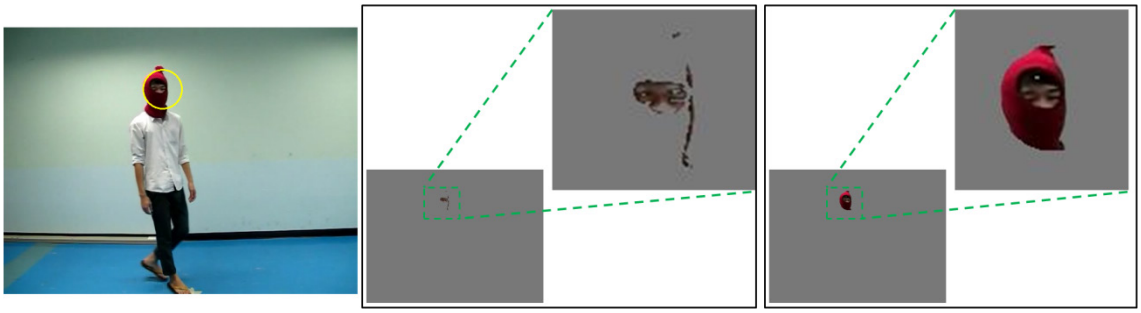

a) Head region b) Skin face data c) Head data

Figure 5 Skin face data and head data.

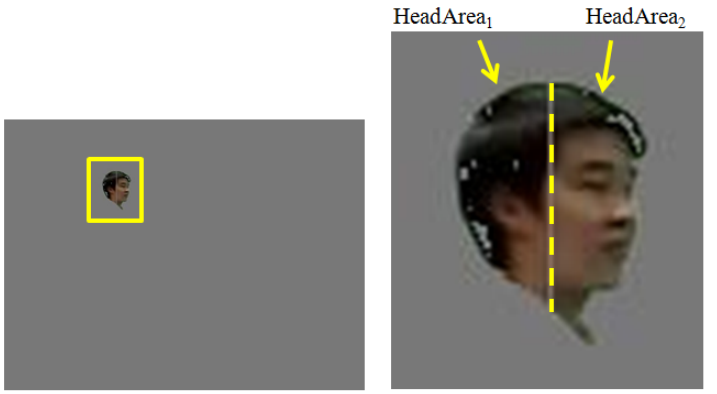

a) head region b) two vertical head regions

Figure 6 The head region divided into 2 vertical regions.

The Mahalanobis distance criteria of Lab, HSV, and YC_BC_R color mode are 5.5, 6.7, and 5.6, respectively. The pixels, which Mahalanobis distance is less than a criterion of each color mode, are defined as a skin color. The Mahalanobis distance of the wall, white shirt or black pants in **Figure 4b** are bigger than the criterion. Finally, only skin data in the head area is defined as skin face color, as shown in **Figure 5**.

For **Figure 5**, the region which the head is located is represented as a yellow cycle (**Figure 5a**). In the head region, skin face color is extracted and enlarged and shown in **Figure 5b**. Head data is also

enlarged and shown in **Figure 5c**. Skin face data and head data are used to compute the skin ratio as explained in next section.

Skin ratio computation and occluded face detection

As this proposed method aims to detect the occluded face from any head viewpoint, the head region s divided into 2 vertical head regions based on head center, as shown in **Figure 6**. A yellow dash line is the head center line. This line passes though head center. The side of the head center line is HeadArea1, and the other side is HeadArea2. This method considers the skin ratio of each vertical region instead of the whole face, as mentioned in previous works [6,7]. The skin ratio of each region is computed as;

$$SKR_i = \frac{SkinArea_i}{HeadArea_i} \times 100\% \quad (3)$$

where SKR_i is the skin ratio for human area number i, i is left or right side head area, *SkinArea* is the number of pixels counted from the skin-color area, and *HeadArea* is the number of pixels counted from the head area.

a) –90 degrees b) –45 degrees c) –22.5 degrees d) 0 degrees

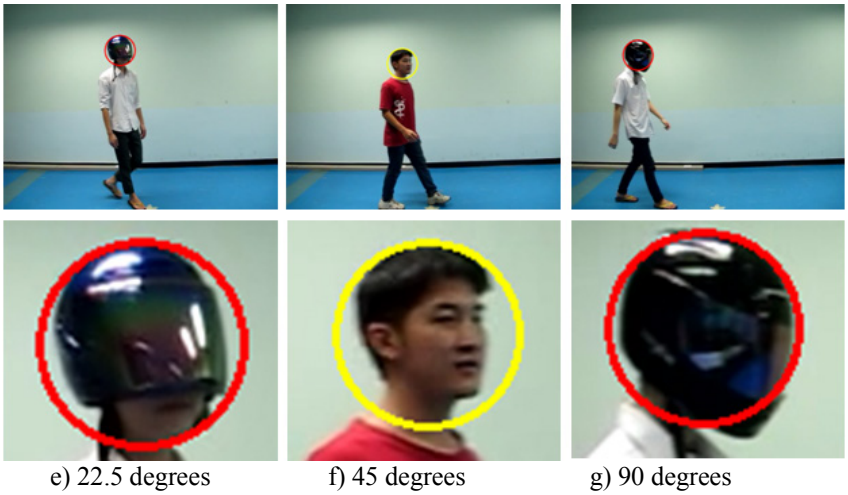

e) 22.5 degrees f) 45 degrees g) 90 degrees

Figure 7 Correct results of occluded and non-occluded face detection.

The first and third row is the whole body image. The head region is enlarged and shown in the second and fourth row. **Figures 7a - 7g** are arranged starting from –90 degrees to +90 degrees around the yaw axis. Non-occluded and occluded faces are presented as the yellow and red cycle, respectively. The obstacle types from **Figures 7a - 7g**, arranged from the left side image to the right side image, are brown, blue and black masks, red and blue helmets, a non-occluded face, and a black helmet, respectively.

The skin ratio is the ratio between the skin area and the head area. A criterion of skin ratio is used to judge the occluded face based on the skin ratio of the vertical region. Based on the pilot test, the criterion ratio is set as 0.5. If a skin ratio of a head region is higher than the criterion, the face is defined as a non-occluded face. If both skin ratios of 2 head regions are lower than the criterion, the face is judged as an occluded face. In the case of capturing a non-occluded face from a side view, one vertical head region has a high skin ratio, and the other has a low skin ratio. Using 2 head vertical regions is appropriate for detecting an occluded face from a side view.

Table 1 Accuracy rate of occluded face detection.

Obstacle	Accuracy	Face capturing angle (Degrees)							
		-90	-45	-22.5	0	22.5	45	90	All viewpoint
Black Helmet	Sample	36	36	36	36	36	36	36	252
	Correct	36	36	36	36	36	36	36	252
	Accuracy	**100**	**100**	**100**	**100**	**100**	**100**	**100**	**100**
Blue Helmet	Sample	36	36	36	36	36	36	36	252
	Correct	36	36	36	36	36	36	36	252
	Accuracy	**100**	**100**	**100**	**100**	**100**	**100**	**100**	**100**
Red Helmet	Sample	36	36	36	36	36	36	36	252
	Correct	31	30	30	33	36	36	36	232
	Accuracy	**86.11**	**83.33**	**83.33**	**91.67**	**100**	**100**	**100**	**92.06**
Black Mask	Sample	36	36	36	36	36	36	36	252
	Correct	36	35	30	35	36	36	36	244
	Accuracy	**100**	**97.22**	**83.33**	**97.22**	**100**	**100**	**100**	**96.83**
Blue Mask	Sample	36	36	36	36	36	36	36	252
	Correct	35	33	33	36	36	36	36	245
	Accuracy	**97.22**	**91.67**	**91.67**	**100**	**100**	**100**	**100**	**97.22**
Brown Mask	Sample	36	36	36	36	36	36	36	252
	Correct	34	28	22	18	31	34	36	203
	Accuracy	**94.44**	**69.44**	**61.11**	**50**	**77.78**	**86.11**	**91.67**	**80.56**
Red Mask	Sample	36	36	36	36	36	36	36	252
	Correct	36	33	33	36	36	36	36	246
	Accuracy	**100**	**91.67**	**91.67**	**100**	**100**	**100**	**100**	**97.62**
Non-occluded Face	Sample	36	36	36	36	36	36	36	252
	Correct	36	36	36	36	36	36	33	249
	Accuracy	**100**	**100**	**100**	**100**	**100**	**100**	**91.67**	**98.81**
Occluded Face	Sample	252	252	252	252	252	252	252	1764
	Correct	244	231	220	230	247	250	252	1674
	Accuracy	**96.83**	**91.67**	**87.30**	**91.27**	**98.02**	**99.21**	**100**	**94.90**
Total Accuracy Rate	Sample	288	288	288	288	288	288	288	2016
	Correct	280	267	256	266	283	286	285	1923
	Accuracy	**97.22**	**92.71**	**88.89**	**92.36**	**98.26**	**99.31**	**98.96**	**95.39**

Experimental results

To evaluate the performance of the proposed method, we measure the occluded face detection accuracy rate. A set of data collected from 36 subjects is used. Images, consisting of faces occluded with helmets and masks, and non-occluded faces, are used in the experiment. Helmet colors consist of red, dark blue and black, while mask colors consist of red, dark blue, brown, and black. A camera captures the whole body into an image sequence format. We capture only one subject in a frame. The camera model is Canon G12. The image size is 640×480 pixels. The frame rate is 30 frames per second.

In this experiment, test data consists of captured subjects turning from –90 degrees to +90 degrees around the yaw axis. The angles of viewpoint, used for accurate measurements, are –90, –45, –22.5, 0, +22.5, +45 and +90 degrees. The results are compared with manual judgments. The sample results are shown in **Figure 7**. **Table 1** summarizes the detection results. **Table 1** shows the total number of test images, correct detection numbers, and accuracy rates. The row of occluded faces in **Table 1** is a summation of helmets and masks with several colors. The total data of occluded and non-occluded faces consists of 2,016 images, as summarized in the row of total accuracy rate. The results show that 93 were wrongly detected. The accuracy rate of occluded face detection is 94.90 %, while the accuracy rate of non-occluded face detection is 98.81 %. The average accuracy rate is 95.39 %.

Almost all accuracy rates are higher than 90 %, except the accuracy rate from some viewpoints of red helmets, black helmets, and brown masks, as shown by the red numbers in **Table 1**. The cause of error will be explained more in the discussion section.

Discussion

In this section, we focus on discussing 6 points: causes of error, low accuracy rates, performance consideration for roll and pitch axis, contributed parameters for performance of the proposed method, limitations for real-life situation, and future performance improvement.

The correct color of cycle on non-occluded faces should be yellow instead of red, while the correct color of cycle on occluded faces should be red instead of yellow. **Figures 8a** and **8b** are examples of wrong classification occurring from light reflection on the face and helmet. **Figures 8c** and **8d** are examples of similarity of color, and marginal miss criterion, respectively.

a) Light reflection on face | b) Light reflection on helmet | c) Similar color | d) Marginal miss criterion

Figure 8 Sample of fault detection results.

Table 2 Causes of occluded face detection error.

Cause of error	Incorrect detection	Percentage (%)
Light Reflection	23	24.73
Similar Color between Skin and Obstacle Color	49	52.69
Error from Marginal Miss Criterion	21	22.58
Total Number of Error	93	100

Causes of error

According to the experimental results, from a total 2,016 test images, 1,923 images were detected correctly, and another 93 images were at fault. We classify the causes of error into 3 cases. This incorrect classification occurs from light reflection, similar color between skin and obstacle color, and error from marginal miss criterion. Similar color between skin and obstacle color caused the biggest error at 52.69 %, with 24.73 % error occurring from light reflection, and 22.58 % error from marginal miss criterion.

Light reflection on the face or obstacle changes the color property of the head region and becomes a brighter area on the face or obstacle, as shown in **Figures 8a** and **8b**. The bright color will be similar to the background. Such pixels will be lost when using the background subtraction technique. The light reflection is a major cause of error for red helmets because the face shield of the red helmet is coated with mercury. Therefore, light refection appeared more easily than other colors of helmet, as shown by the low accuracy for the red helmet in **Table 1**. For future improvement, a human tracking system will be applied as an assistance technique, to extract the human head region more accurately.

Regarding similarity of color between skin and obstacle color, there are many errors in sample fault detection when using the brown color mask in the experiment, as also shown in the low accuracy rate in **Table 1**. An example of incorrect brown mask detection is shown in **Figure 8c**. The brown color of this mask is similar to skin color. Both the brown mask and the skin are extracted in the skin extraction process. Therefore, additional information as to the different shape of head with and without obstacle will be needed for future performance improvement.

As we set a criterion for the skin ratio, obviously, the skin ratio of some test data will be of marginal miss criterion. **Figure 8d** shows a sample of fault detection in the case of marginal miss criterion. For improving performance, a pattern recognition technique, such as a support vector machine, will be used to include additional information from the shape of head with and without obstacle.

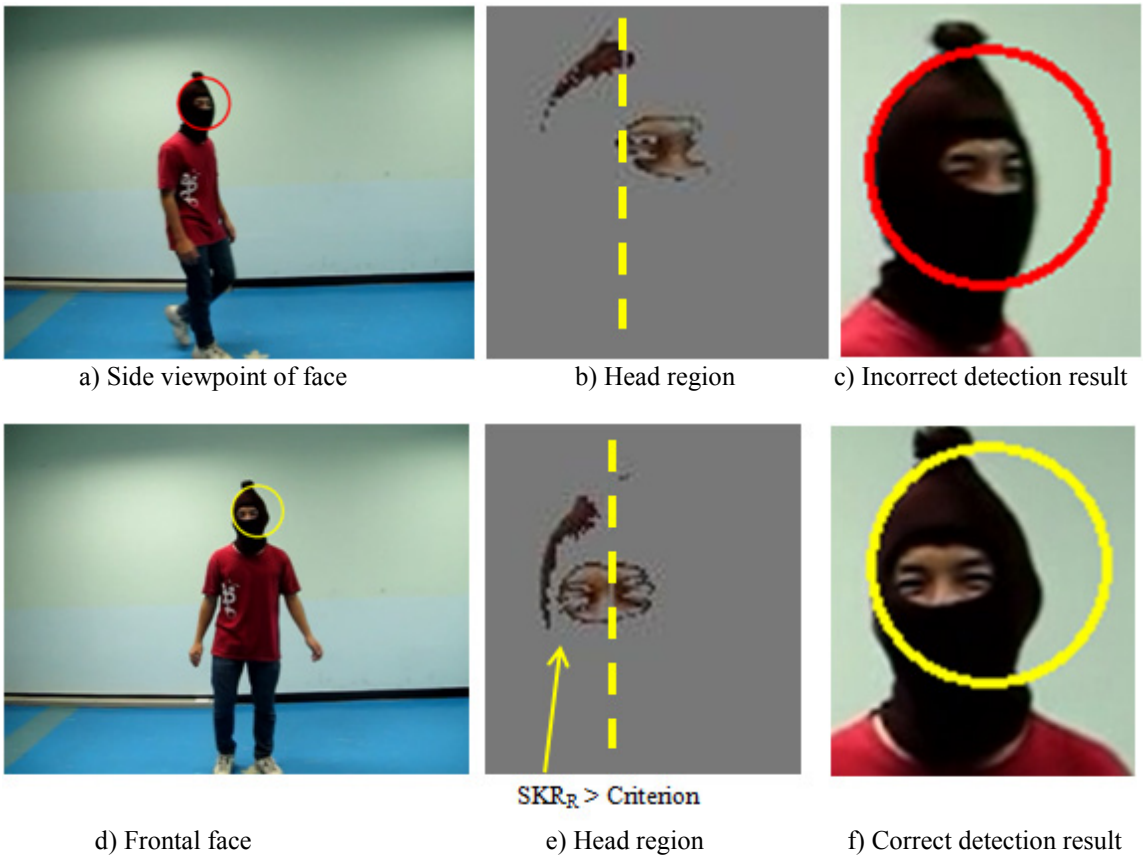

a) Side viewpoint of face b) Head region c) Incorrect detection result

d) Frontal face e) Head region f) Correct detection result

Figure 9 Comparison of skin area extraction between correct and incorrect detection results.

Low accuracy rate

As shown in **Table 1**, low accuracy rate occurred especially in the case of a face with a brown mask for face orientation between –22.5 degrees and +22.5 degrees. For a narrow angle of face orientation from frontal face with mask, obviously, the skin area is bigger than the side viewpoint, as shown in **Figure 9**. Incorrect skin area is also extracted, as shown in **Figures 9b** and **9e**. The incorrect skin area is a part of brown mask. Therefore, the skin ratio becomes bigger for both frontal face and side viewpoint face. For the frontal occluded face, the skin ratio is normally a marginal fail for all colors of mask. In the case of brown masks, incorrect skin area as a part of mask is also extracted. The skin ratio marginally passes the criterion. Occluded face detection is then judged as a normal face. In the case of a side viewpoint of a face with a brown mask, skin ratio with incorrect skin area is not big enough to pass the criterion. It is still judged correctly as an occluded face.

Figures 9a - 9c shows occluded face data from a side viewpoint. **Figures 9d - 9f** shows occluded face data from a frontal viewpoint. The detection result of the side viewpoint is correct, while the detection result of the frontal viewpoint is incorrect.

Performance consideration for roll and pitch axis

This experiment aims to study performance of the occluded face detection method in the case of a head pose that varies in roll and pitch. Data is collected from 12 subjects. The experiment captures the face image at angles of –22.5, –45, +22.5 and +45 degrees rotated around the roll and pitch axis. The obstacle type, its color, camera setting condition, and envelopment are the same as the experiment of the

performance evaluation in the yaw axis. From 760 images, 663 images are correct and 97 images are incorrect. The average accuracy rate is 87.24 %. The sample result is shown in **Figure 10**. They show the feasibility of this method when the head pose varies in roll and pitch.

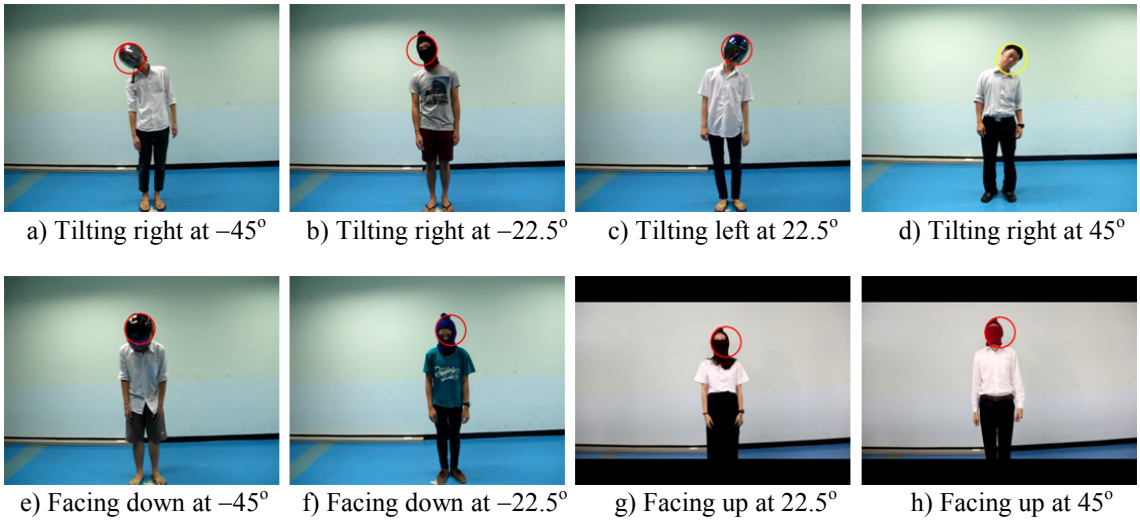

a) Tilting right at –45° b) Tilting right at –22.5° c) Tilting left at 22.5° d) Tilting right at 45°

e) Facing down at –45° f) Facing down at –22.5° g) Facing up at 22.5° h) Facing up at 45°

Figure 10 Occluded and non-occluded face detection for face rotation in the roll and pitch axis.

Contributed parameters for performance of the proposed method

In the occluded face detection method section, the 2 parameters contributing to accuracy rate are: the Mahalanobis distance criterion, and the skin ratio criterion. If the Mahalanobis distance criterion is too big, other pixels which are not skin will also be extracted in the skin extraction step. In the case of the Mahalanobis distance criterion being too small, some skin pixels will not be extracted in the skin extraction step. The Mahalanobis distance criterion impacts the performance of skin extraction. For the skin ratio criterion, if it is too big, a normal face will be judged as an occluded face, while if it is too small, an occluded face is judged as a normal face.

Limitations for real-life situations

As the proposed method focuses on occluded face detection, images of one person are used in this method in order to achieve the research goal. For real-life situations, 2 limitations of the proposed method are considered: occlusion from more than one person, and multiple-masked faces in an image. To solve these limitations, a method of human detection and tracking is needed in the preprocessing process, and our proposed method will be used to detect the occluded face of each person. Finally, this algorithm will be able to detect the occluded face from multiple people with multiple-masked face.

Future Performance Improvement

Principle component analysis and support vector machines are effective techniques for classification; they have also been applied in the methods of references [2,3]. For our future work, we plan to improve the accuracy of our method by using principle component analysis and support vector machines. The head region will be divided into multiple sub-regions, which means more than 2 head areas. PCA will define significant sub-regions, and SVM will then be used to maximize the accuracy. This is the plan to improve performance.

Conclusions

This paper proposes a new method to detect occluded faces from any viewpoint of a face by using Hough transform and the skin ratio. The proposed method classifies non-occluded and occluded face based on 2 skin ratios in the head region. The whole body of the subject is captured in the test data set. The head pose varies from –90 degrees to +90 degrees in yaw. The obstacles used in the experiment are helmets and masks of different colors. The total test data consists of 2,016 images. 1,923 images are detected correctly. The accuracy rate of occluded face detection is 94.90 %, while the accuracy rate of non-occluded face detection is 98.81 %. The average accuracy rate is 95.39 %. Lighting reflection, similarity of color between skin and obstacle, and marginal miss criterion cause detection faults. This method also performs satisfactorily for head poses in roll and pitch. The advantage of this method is that this is first method to detect an occluded face from any viewpoint of the head from –90 degrees to +90 degrees in yaw with a satisfactory accuracy rate.

For future work, the accuracy rate will be improved in 3 ways: extracting the human head region more exactly, by a human tracking system, additional information, such as the classification of different shapes of heads with and without obstacles, and using higher performance techniques for classification, such as principle component analysis and support vector machines.

Acknowledgements

This research was financially supported by the Faculty of Engineering, Srinakharinwirot University, Thailand. The author would like to thank all of the students in the Department of Biomedical Engineering, Faculty of Engineering, Srinakharinwirot University, for their assistance in database correction.

References

[1] AM Martinez and R Benavente. *The AR Face Database*. CVC Technical Report 24, 1998.
[2] R Min, A D'angelo and JL Dugelay. Efficient scarf detection prior to face recognition. *In*: Proceedings of the 18th European Signal Processing Conference, Aalborg, Denmark, 2010, p. 259-63.
[3] GN Priya and RSDW Banu. Detection of occluded face image using mean based weight matrix and support vector machine. *J. Comput. Sci.* 2012; **8**, 1184-90.
[4] SM Yoon and SC Kee. Detection of partially occluded face using support vector machines. *In*: Proceedings of the IAPR Workshop on Machine Vision Applications, Nara, Japan, 2002, p. 546-9.
[5] CY Wen, SH Chiu, J Liaw and C Lu. The safety helmet detection for ATM's surveillance system via the modified Hough transform. *In*: Proceedings of the IEEE 37th Annual 2003 International Carnahan Conference on Security Technology, Taipei, Taiwan, 2003, p. 364-9.
[6] DT Lin and MJ Liu. Face occlusion detection for automated teller machine surveillance. *Adv. Image Video Tech.* 2006; **4319**, 641-51.
[7] G Kim, JK Suhr, HG Jung and J Kim. Face occlusion detection by using B-spline active contour and skin color information. *In*: Proceedings of the 11th International Conference on Control Automation Robotics & Vision, 2010, p. 627-32.
[8] J Chiverton. Helmet presence classification with motorcycle detection and tracking. *IET Intell. Transport Syst.* 2012; **6**, 259-69.
[9] T Charoenpong. Face occlusion detection by Ellipse fitting and skin color ratio. *In*: Proceedings of the Burapha University International Conference, Chonburi, Thailand, 2013, p. 1145-51.
[10] T Charoenpong, C Nuthong and U Watchareeruetai. A new method for occluded face detection from single viewpoint of head. *In*: Proceedings of the 11th International Conference on Electrical Engineering/Electronics, Computer, Telecommunications and Information Technology, Nakhon Ratchasima, Thailand, 2014, p. 1-5.

[11] S Thakur, S Paul, A Mondal and SW Das. Face detection using skin tone segmentation. *In*: Proceedings of the 2011 World Congress on Information and Communication Technologies, Mumbai, 2011, p. 53-60.
[12] P Ng and CM Pun. Skin color segmentation by texture feature extraction and K-mean clustering. *In*: Proceedings of the 3rd International Conference on Computational Intelligence, Communication Systems and Networks, Bali, 2011, p. 213-8.
[13] MA Zia, U Ansari, M Jamil, O Gillani and Y Ayas. Face and eye detection in images using skin color segmentation and circular Hough transform. *In*: Proceedings of the International Conference on Robotics and Emerging Allied Technologies in Engineering, Islamabad, 2014, p. 211-3.
[14] MM Hasan and MF Hossain. Facial features detection in color images based on skin color segmentation. *In*: Proceedings of the International Conference on Informatics, Electronics & Vision, Dhaka, 2014, p. 1-5.
[15] S Singh, DS Chauhan, M Vatsa and R Singh. A robust skin color based face detection algorithm. *Tamkang J. Sci. Eng.* 2003; **6**, 227-34.